Application of neural network for airship take-off and landing system by buoyancy change

Yongjin Chang*, Guiaee Woo**, Jongkwon Kim***, and Kyeumrae Cho****

* Department of Aerospace Engineering, Pusan Nat'l University, Busan, Korea
(Tel : +82-51-510-3036; E-mail: yjchang@pusan.ac.kr)
** Department of Aerospace Engineering, Pusan Nat'l University, Busan, Korea
(Tel : +82-51-510-3036; E-mail: lohen99@dreamwiz.com)
*** Department of Aerospace Engineering, Pusan Nat'l University, Busan, Korea
(Tel : +82-51-510-3036; E-mail: joinkiss@korea.com)
**** Department of Aerospace Engineering, Pusan Nat'l University, Busan, Korea
(Tel : +82-51-510-3036; E-mail: krcho@pusan.ac.kr)

Abstract: For long time, the takeoff and landing control of airship was worked by human handling. With the development of the autonomous control system, the exact controls during the takeoff and landing were required and lots of methods and algorithms were suggested. This paper presents the result of airship take-off and landing by buoyancy control using air ballonet volume change and performance control of pitch angle for stable flight within the desired altitude. For the complexity of airship's dynamics, firstly, simple PID controller was applied. Due to the various atmospheric conditions, this controller didn't give satisfactory results. Therefore, new control method was designed to reduce rapidly the error between designed trajectory and actual trajectory by learning algorithm using an artificial neural network. Generally, ANN has various weaknesses such as large training time, selection of neuron and hidden layer numbers required to deal with complex problem. To overcome these drawbacks, in this paper, the RBFN (radial basis function network) controller developed.

Keywords: Pressurizing Capacity, Artificial Neural Network, Takeoff and Landing, Radial Basis Function Network

1. INTRODUCTION

Ballonet of non-rigid type airships is expanded or shrunk by changing of pressure height. Ballonet is stressed by internal pneumatic expansion or shrinking due to rising pressure height. If it is not emitted gas from the air ballonet when airship climbs, hull of airship is suffered large stress. On the contrary, when airship descents the hull of airship is suffered the stress by shrunken gas. And it is hard to maintain shape of airship. So, most of the non-rigid type airship applies ballonet system such as fig. 1. An air ballonet acts to inhale or to flow out air by changing due to expanding or shrinking internal gaseous volume. In this paper, pressurizing capacity is calculated and estimated the volume flow late. And then that result used in the altitude control. Finally, control of pitch angle for stable flight is performed within the desired altitude. For the complexity of airship's dynamics, firstly, simple PID controller was applied. Due to the various atmospheric conditions, this controller didn't give satisfactory results. Therefore, new control method was designed to reduce rapidly the error between designed trajectory and actual trajectory by learning algorithm using an artificial neural network.

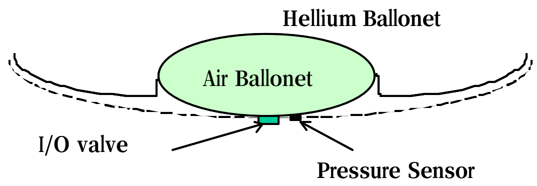

fig 1 Airship Ballonet system

2. AIRSHIP BALLUNET

2.1 Pressurizing Capacity

Pressurizing capacity means the bulk of air or gas to flow out or supply per unit time. All gas relation formula is derived in ESDU 68046, because ESDU 68046 provides tables of the properties of the International Standard Atmosphere. First of all, the volume change of helium and that of air ballonet relations to altitude was derived of based on following Gas Law.

$$\frac{P_0 V_0}{T_0} = \frac{P_s V_s}{T_s} \tag{1}$$

subscripts,

$_0$ = Standard condition at sea level

$_s$ = Properties relation to height

The temperatures used in following formula are in $^\circ K$ where the ice point is $273.15^\circ K$. Atmospheric properties are defined by temperature-height profiles with the general formula;

$$T_s = T_0 + A \cdot H \tag{2}$$

here, T_0 = $273.15^\circ K$ (temperature at sea level)

A = -0.0065 (temperature gradient)

The pressure P_s at a pressure height H_p is given by

$$P_s = P_0 \left(\frac{T_s}{T_0} \right)^{\frac{-g_0}{A \cdot R_A}} \tag{3}$$

here, P_0 = 101325 N/mm^2

g_0 = 9.8 m/s^2

R_a = 287.05287 $N \cdot m / kg \cdot K$

Helium and air volume change are rewritten as eqn. (4).

$$V_s = V_0 \left(\frac{T_s}{T_0} \right)^{-1-\frac{g_0}{A \cdot R_A}} \tag{4}$$

By the eqn. (4), internal pneumatic expansion and shrinking volume can be calculated and then the volume flow late of air required determined as eqn. (5).

$$Q_{vol}=\frac{(\Delta V_{gellium}+\Delta V_{air})}{\Delta h}\times \mathrm{ROC} \quad (5)$$

here, ROC =3 m/s (the rate of climb)

Using above gas eqn. (1)-(5), volume flow late for 11m-airship was calculated as fig 2.

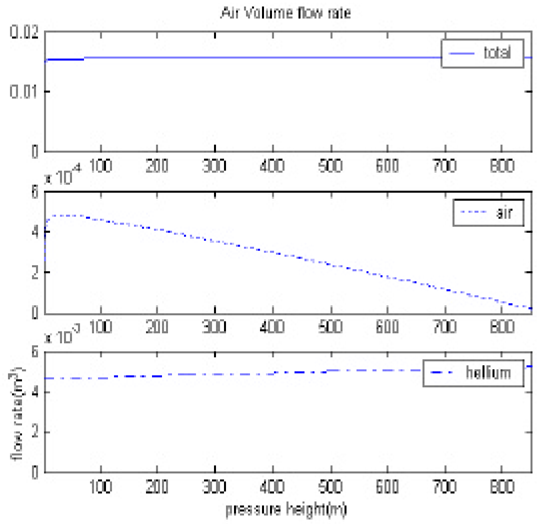

fig 2. Air volume flow rate per unit time

Fig 3. is a pressure height and lift relation curve. The dot line is the case of no emission and solid line is the use of emission. Known from the figure, the net lift is increased maximum 13% by the air emission. Because 11m-airship is limited by air ballonet volume, lift change is not occurred over height 880m.

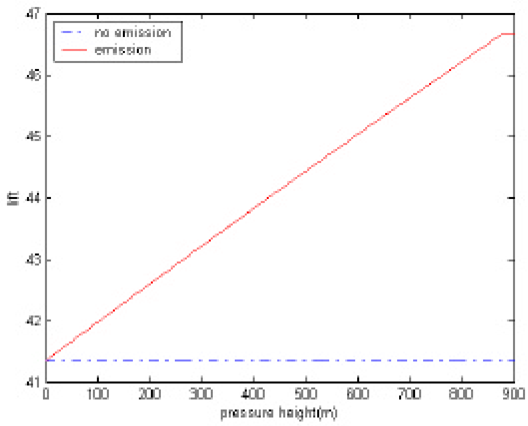

fig 3. Lift variation

3. AIRSHIP DYNAMICS

3.1 Longitudinal dynamics

In this section we briefly review the basic nonlinear dynamic model representing the airship. The equations of motion in this paper are referred general dynamics.

Airship dynamics are a complicated with the 6-degree of freedom, but in this paper only used 2-axis force (axial and normal force) and pitching moment equation because of researching motions of a longitudinal direction. It assumed that thruster was symmetric and generated the same magnitude in port and starboard. The dynamic equations applied this study are as follows.

$$m_x\dot{u}+m_zqw-m\ rv-ma_x(q^2+r^2)+(ma_z-\overset{\circ}{X}_{\dot q})\dot q+ma_zpr = X_{ext}$$

$$m_z\dot{w}+m_ypv-m_xqu-(ma_x-\overset{\circ}{Z}_{\dot q})\dot q+ma_xrp-ma_z(p^2+q^2) = Z_{ext}$$

$$I_{yy}\dot q+pr(I_{xx}-I_{zz})+I_{xz}(p^2-r^2)-ma_x(\dot w+pv-qu)+ma_z(\dot u+qw-rv)-\overset{\circ}{M}_{\dot u}\dot u-\overset{\circ}{M}_{\dot w}\dot w=M_{ext} \quad (6)$$

$$X_{ext}=X_A+l_{31}(W-B)+2T\cos m$$

$$Z_{ext}=Z_A+l_{33}(W-B)-2T\sin m$$

$$M_{ext}=M_A+(l_{31}a_z-l_{33}a_x)W+2T(d_z\cos m-d_x\sin m)$$

Here, W is airship's total weight, B is buoyancy force, l_{ij} is direction cosine vector components and T is the thrust that is located in gondola having m angle to the horizontal axis.

In takeoff and landing procedure, airship height is essentially affected by buoyancy change and control surface input to control attitude doesn't applied. A velocity and an attitude control are performed after climbing.

3.2 Motor & control system block diagram

The motor composing a pressurizing system can be represented using a general dc motor dynamics.

$$J_m\ddot q_m+(b+\frac{K_tK_q}{R_a})\dot q_m=\frac{K_ti_a}{R_a}V_a \quad (7)$$

where, $b=0.001\ [N\cdot m\cdot s]$

$K_t=1\ [N\cdot m/A]$

$K_q=0.02\ [V\cdot s]$

$R_a=10\ [\Omega]$

$J_m=0.01\ [kg\cdot m^2]$

Control system block diagram is shown fig 4. The main control concept is to minimize an error with a designed reference input.

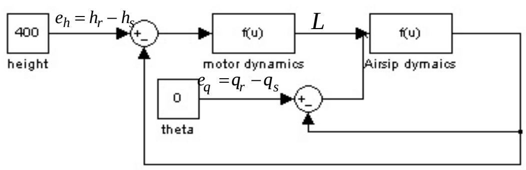

fig 4. Total close loop block diagram (without controller)

Here, e_h is height error between desired latitude and output and e_q is pitch angle error. L is lift after emission by motor control.

4. DEVELOPMENT OF NEURAL NETWORK

Fig. 5 illustrates an RBFN with inputs x_1, ..., x_n and output $\hat{y}$. The arrows in the figure symbolize weight value parameters in the network. The RBFN consists of one hidden layer of basis functions, or neurons. At the input of each neuron, the distance between the neuron center and the input vector is calculated. Then, the output of the neuron is got applying the basic function to this distance. The RBFN output is formed by a weighted sum of the neuron outputs and the unity bias shown.

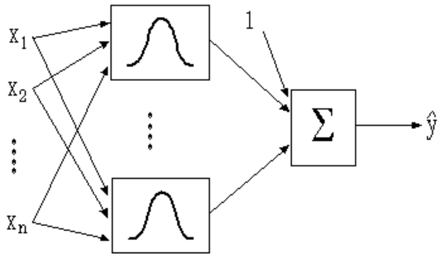

fig 5. RBFN basic concept diagram

The architecture of RBFN is determined from the learning algorithm it is used. Considering the size of the training set we have, the function *newrb* in MATLAB Neural Network Toolbox was adopted. This function iteratively creates a radial basis network, one neuron at a time. The weight value of the neuron is one sample in the training set. Neurons are added to the network until the sum-squared error falls beneath an error goal. In our application, Gaussian functions were utilized as the radial basis functions for the hidden layer neurons. The most important parameter to design a RBFN is the bias for the radial basis neurons. The bias should be small enough so that the active input regions of the radial basis neurons overlap enough to make the network function smoother and results in better generalization for new input vectors.

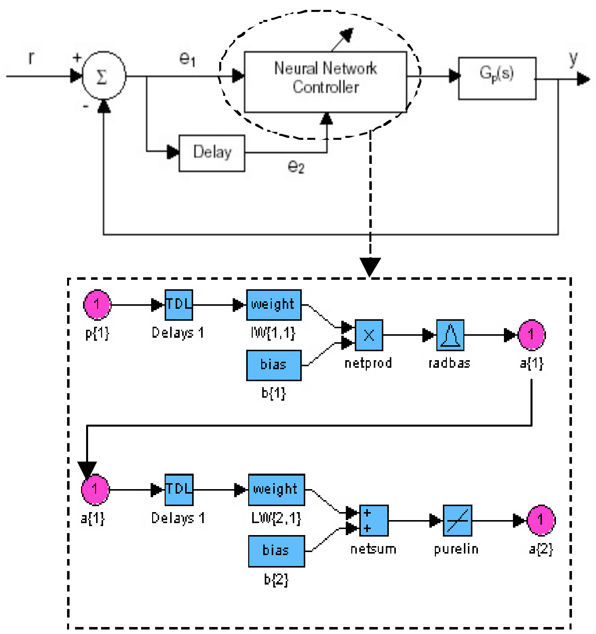

fig 6. System block diagram with RBFC

However, bias should not be so small that each neuron is effectively responding in the same, large, area of the input space. Therefore, the similar cross-validation procedure was applied to choose an appropriate bias for each network in primary and secondary fault modules. After all the parameters were determined, the networks were trained and tested. In this paper, spread of radial basis function was set 0.2 and mean squared error goal is 0.02. The weight and biases of each neuron in the hidden layer define the position and width of a radial basis function. The number of hidden layer is one and the layer has 9 neurons.

5. SIMULATION RESULTS

If rate of climb and descend is set to 3 m/s, it has to inhale and flow out the air a mount of 0.016 m^3 per second in take off and landing procedure of airship. The value of variables and parameters used airship is set as Table 1.

Table 1. Value of variables and parameter

Variable		Value
Length [m]		11
Width [m]		3.6
Weight [kg]	Ballonet	20
	Control surface	4.5
	Gondola	20
Initial Volume [m^3]	Helium	39.15
	Air	4.35
Inertia Moment [$kg \cdot m^3$]	I_{xx}	151.56
	I_{yy}	248.35
	I_{zz}	201.44
	I_{xz}	0.867

PID control method was compared with RBFN in simulation. The desired altitude of 11m-airship is 400m, attitude control for stable flight must to be assured the performance for the additional purposes (filming, observation, etc.) in this altitude. In fig 7, 2 method of control to climb to 400m was shown good results that PID controller is better than RBFN (from climb to cursing flight) to maintain the altitude.

To design PID controller, let the error value e be the difference the reference value y_r from current value y, and use the control input u to minimize the error. Table 2 is shown PID controller gain values.

$$e = y_r - y$$
$$u(t) = K_p e(t) + K_i \int e dt + K_d \frac{de}{dt} \quad (8)$$

Here, K_p is the proportional gain, K_i the integration, and K_d the derivation. Take the Laplace transfer of Eq.(8).

$$\frac{u(s)}{e(s)} = K_p (T_d s + 1 + \frac{1}{T_i s}) \quad (9)$$

Table 2. PID Controller Gain Value

K_p	T_i	T_d
10	5	0.5

But fig. 8 is shown the different results for the pitch angle to maintain the target altitude. In the case of PID controller, pitch angle rapidly changes and doesn't recover to target value (0°). But RBFN controller traces the reference value. In the fig. 9, AOA (Angle of attack) shows the similar results compared with those of the fig. 8.

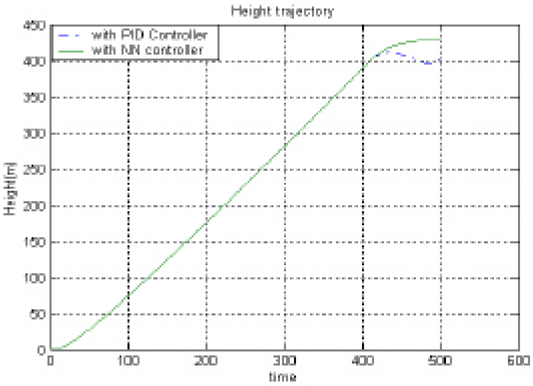

fig 7. Height trajectory

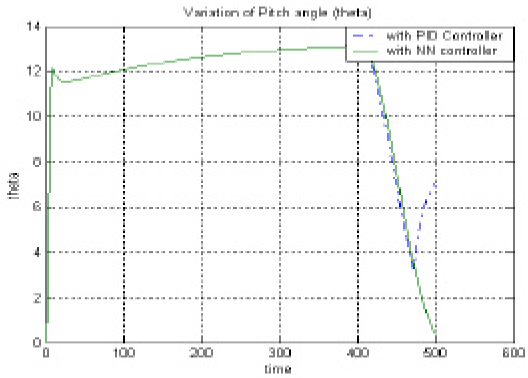

fig 8. Variation of Pitch angle

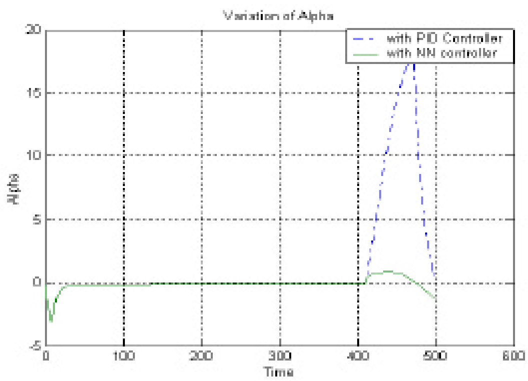

fig 9. Variation of AOA (Angle of attack)

6. CONCLUSION

In this paper, firstly, pressurizing capacity to keep hull shape and internal pressure is calculated. With this, air volume for inhaling or emitting by ROC (the rate of climb) is computed. And then controller is designed to keep the desired altitude by two methods (PID, RBFN). PID controller is better than RBFN (from climb to cursing flight) to keep altitude, but pitch angle and AOA rapidly changes and doesn't follow the reference value. Therefore, RBFN is more stable method for the altitude control.

EFERENCES

[1] S.B.V. Gomes, "An Investigation of the Flight Dynamics of Airship with Application to the YEZ-2A", *Ph.D. thesis*, College of Aeronautics, Cranfield Institute of Technology, Cranfield, 1990.

[2] G.A. Khoury and J.D. Gillett, *Airship Technology*, Cambridge University Press, 1999.

[3] M.V.Cook, J.M. Lipscombe, and F. Goineu, "Analysis of the stability modes of the non-rigid airship", *Aeronautical Journal*, pp.279-290, June 2000.

[4] S. H. Oh, D. M. Kim, Y. K. Lee, and J.W. Lee, "Estimation of Pressurizing Capacity for 50m Class Unmanned Airship", *Annual meeting of KSAS*, pp.242-245. 2002

[5] G. A..Woo, I. H. Park, S. J. Oh, and K.R. Cho, "Dynamic response and control of airship with gust", *journal of KSAS*, Volume 30, No.6, pp.69-77.

[6] D.K.Chaturvedi, R.Chauhan, P.K.Kalra, "Application of generalized neural network for aircraft landing control system," *Soft Computing 6*, pp 441-448, Springer-Verlag, 2002

[7] K.Chulhwan, W. Guiaee,O. Saejong, and C. Kyumrae, L. Daewoo, "Dynamic Response of An Airship at Cruising", *2001 ICASS*, pp 1110-1112

[8] K. S. Narendra and K. Parthasarathy, "Identification and Control of Dynamical Systemsusing Neural Networks", *IEEE Transactions on Neural Networks*, Vol. 1, pp 1-27, 1990.

[9] M.Norgaard, O.Ravn, N.K.poulsen and L.K.Hansen, *Neural Networks for Modeling and Control of Dynamics Systems*, Springer, 2001

[10] M.Jerzy, O.Zbigniew, Advanced Control with Matlab and Silulink, Ellis Horwood, 1995

[11] E.C. de Paiva, J.R.H Carvalho, P.A.V. Ferreira, and J.R. Azinheria, "An H_2/H_∞ PID Heading Controller for AURORA-I Semi-Autonomous Robotic Airship", *Proc. of the 14 Lighter-Than-Air Technical Committe Convention & Exhibition*, Akron, Ohio, USA, July 15-19, 2001